Chapter 3

Smart Home Energy Management System (SHEMS) under False Data Injection (FDI) Attack

3.1 Introduction

The electricity demand is increasing rapidly with the increase in the population density, diversification of city limits, and environmental constraints. For this, there is a need to develop the power grid into a more secure and modern smart grid incorporating Information and Communication Technology (ICT), two-way communication and intelligent technologies. Demand-Side Management (DSM) is used by utilities to minimize the energy cost and effective utilization of energy resources with the help of Demand Response (DR) programs. To reduce the consumption of conventional energy, Renewable Energy Sources (RESs) such as roof-top solar PV panels and small wind turbines are being installed at the residential buildings. Battery Storage System (BSS) can be used to reduce fluctuations due to the intermittent nature of RESs. It is expected that the integration of distributed energy sources will affect the dynamic pricing of electricity. There is an upsurge of technological advancement of the residential buildings to become smarter with the wide use of smart components and integration of IoT. To get maximum benefit of Real Time Price (RTP) and to achieve maximum utilization of RESs, smart components needs to be properly scheduled.

As Smart Homes (SHs) are integrated with ICT with intelligence techniques, they are prone to cyber-attack. Attacker may be a consumer himself (in case of single SHEMS) or a SH user (in SH community system). In such cases attacker normally injects false data. Here it's considered that the attacker is capable of injecting false data into the smart meter so as to create an error vector based on actual and forecasted data for a particular interval.

It is worth mentioning that the mitigation of impact of cyber-attack in the scheduling of smart home architecture has not been widely explored in previous literature. In this chapter, an attempt has been made to formulate the objective function with inclusion of FDI attack constraints on the scheduling process and this chapter also aims to formulate FDI-attack resilient scheduling considering prices and battery degradation cost in the objective function. The work presented in this chapter considers FDI attack modelled using Gaussian Process Regression (GPR) method which is difficult to detect using widely used detection mechanisms. The key contribution of this chapter can be summarized as follows.

- Formulation of an optimization problem in SHEMS has been done to minimize the energy cost and battery degradation cost of smart home considering the user comfort and dynamic demand response.

- Modeling of FDI attack with GPR method has been done considering three month historical data and an initial attack vector.

- An FDI attack resilient scheduling has been developed based on predicted bill calculated with the use of reduced scenario tree.

3.2 System Architecture

In this chapter, it has been assumed that SHs are using the following three types of loads: (*i*) Unschedulable Noninterruptible Loads (UNLs), (*ii*) Temperature Dependent Loads (TDLs) and (*iii*) Scheduable Loads (SLs). UNLs such as light, fan, laptop, TV, speaker and mobile charger etc. are fully dependent on comfort and interest of consumers. As operating time of this type of load depends on the desire and comfort of the consumers, the SHEMS has no control over the scheduling of the UNLs. When the total power demand of UNLs exceeds the predefined limit set by the consumer, smart UNLs module communicates a warning message to the SHEMS.

TDLs are the temperature controlled devices such as air conditioners, refrigerators, water heaters and space heaters. These loads operate in temperature range pre-set by user and a pre-specified settings by the manufacturer. The on/off status of TDLs depends on the violation of the pre-set temperature ranges.

In the present scenario, the residential consumers use RESs such roof top solar PV panels and roof top small wind turbine to reduce their electricity bill and dependency on the utility. Due to the intermittent nature of the RES, SHs use battery back up to enhance the reliability of the entire system. A SHEMS based architecture is proposed as per Figure 3.1 to manage the operation of domestic loads as well as battery operation (charging, discharging, floating) in such way that the energy generation by RES can be used effectively. This architecture comprises of smart appliances (UNLs, TDLs, DLs), solar PV, wind turbine, smart power converters, smart meters, LAN, controller and Energy Management Unit (EMU).

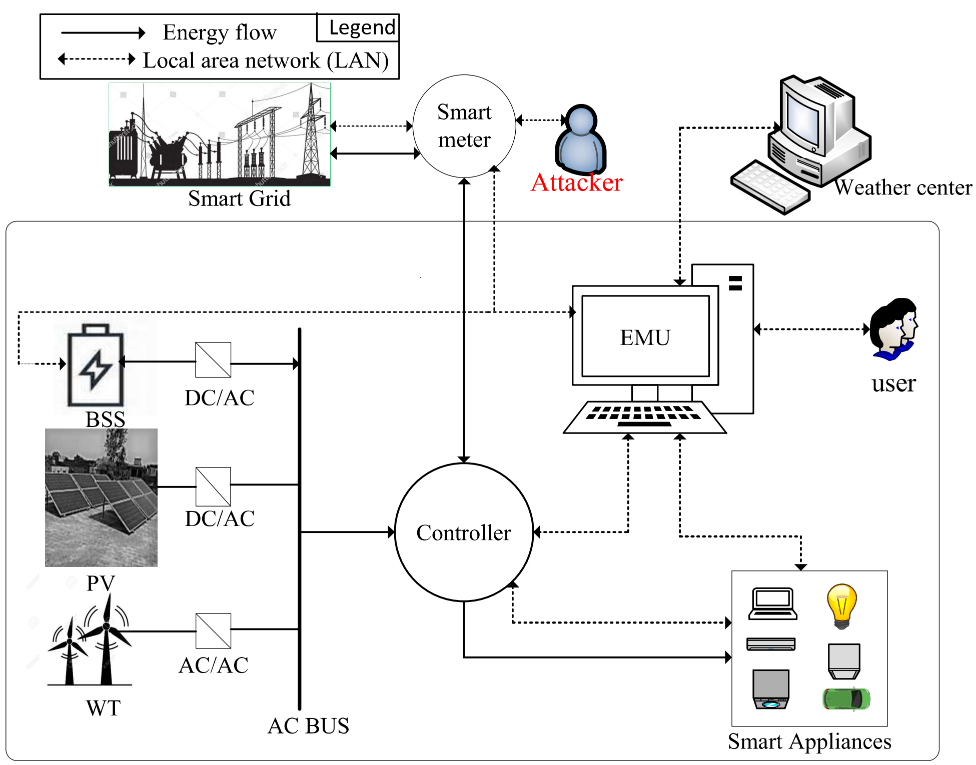

Figure 3.1: System Architecture

The SHEMS is capable of receiving updates of electricity price, along with Maximum Demand Limit (MDL) and Power Export Limit (PEL) from the utility company through the LAN. This is achieved with the help of smart meters which have the capability to communicate with the utility.

3.3 Problem Formulation

3.3.1 Energy Cost and Battery Degradation Cost Minimization

In this chapter, the objective is to minimize battery degradation cost and the energy cost through scheduling of the SLs and TDLs considering Real-Time Pricing (RTP). The main constraints involved in present problem are related to the consumer behaviour which is reflected in terms of operation and duration of devices, availability of renewable power generation, battery storage limits and MDL. A 15 min time interval is considered for 24 hour scheduling.

To minimize the energy cost and battery degradation cost, the objective function can be written as,

$$min\Big(\sum E(t) \times \lambda(t) + C_{cyc}(t)\Big), \tag{3.1}$$

The first term of the objective function is the energy cost and the second term, $C_{cyc}(t)$, is the degradation cost of the battery. The energy cost during a time interval t depends on the net energy consumption during that time interval, $E(t)$, and the price of electricity, $\lambda(t)$. The net energy consumption, $E(t)$, depends on the energy consumption of different loads (UNLs, TDLs, and SLs), energy exchange with BSS, and RESs generation during the time interval t. The $E(t)$ can be defined as,

$$E(t) = (P_{UNLs}(t) + P_{TDLs}(t) + P_{SLs}(t) + P^{ch}(t) - P^{dis}(t) - P^{r}(t))(\Delta t/60). \tag{3.2}$$

Here, $P_{UNLs}(t)$, $P_{TDLs}(t)$, and $P_{SLs}(t)$ are respectively the power demand of the UNLs, TDLs and SLs during the interval t. $P^{r}(t)$ is the expected renewable generation during the interval t and $P^{ch}(t)$ and $P^{dis}(t)$ are the charging and discharging power of battery during the interval t.

Since UNLs can neither be interrupted nor be shifted from one time period to another, the SHEMS don't have control on these loads. SHEMS can only communicate a warning signal if the total demand exceeds the MDL. The total energy consumption, $P_{UNLs}(t)$, of UNLs is the sum of power consumption of each UNL.

The SHEMS controls the ON/OFF status of Temperature Dependant Loads (TDLs) according to the range of temperature pre-set by the consumer. So the SHEMS have the flexibility to switch ON/OFF the TDLs and the power demand of TDLs can be expressed as,

$$P_{TDLs}(t) = P_{rrf} \times S_{rf}(t) + P_{rac} \times S_{ac}(t). \tag{3.3}$$

Here, P_{rrf} and P_{rac} are the rated power of refrigerator and rated power of air conditioner, respectively. $S_{rf}(t)$ and $S_{ac}(t)$ are the ON/OFF status of refrigerator and air conditioner at time interval t. The equations (3.4) and (3.5) represent the toggling condition of $S_{rf}(t)$ and $S_{ac}(t)$, respectively.

$$S_{rf}(t) = \begin{cases} 0, & \text{if } T \leq T^{in,min}, \\ 1, & \text{if } T \geq T^{in,max}. \end{cases} \tag{3.4}$$

$$S_{ac}(t) = \begin{cases} 0, & \text{if } T \leq T_r^{min}, \\ 1, & \text{T} \geq T_r^{max}. \end{cases} \tag{3.5}$$

The power consumption of schedulable loads, $P_{SL}(t)$, can be defined as,

$$P_{SL}(t) = \sum_{a_s=1}^{A} S_{a_s}(t) \times P_{a_s}, \tag{3.6}$$

where, P_{a_s} is the rated power of appliance a. The operating state of a_s^{th} SL can be represented by a binary variable, $S_{a_s}(t)$, as follows.

$$S_{a_s}(t) = \begin{cases} 1, & \text{for ON state} \\ 0, & \text{for idle state.} \end{cases} \tag{3.7}$$

Since the SLs have pre-defined duration of operation within a time range, each appliance, a_s, must satisfy following constraint.

$$d_{a_s} = \sum_{t=tin_{a_s}}^{tout_{a_s}} S_{a_s}(t). \tag{3.8}$$

Here $[tin_{a_s}, tout_{a_s}]$ is the time range operation of appliance, a_s, and d_{a_s} is the pre-defined duration of operation to complete the task.

The net power demand of a smart home should be less than the MDL, P_{mdl}, as given in the following constraint.

$$P_{UNLs} + P_{TDLs} + P_{SLs} + P^{ch}(t) - P^{dis}(t) - P^{r}(t) \leq P_{mdl}. \tag{3.9}$$

The constraint (3.10) restricts the operating temperature, $T_{a_{td}}(t)$, within the pre-set range for ${a_{td}}^{th}$ TDLs.

$$T_{a_{td}}^{min} \leq T_{a_{td}}(t) \leq T_{a_{td}}^{max}, a_{td} = 1, 2, ... \tag{3.10}$$

The operation of BSS are constrained by equations (3.11)-(3.15) as follows.

$$SOC(t+1) = (1-\sigma) \times SOC(t) + (\Delta t/60) \times (\eta^{ch} P^{ch}(t) - P^{dis}(t)/\eta^{dis}), \tag{3.11}$$

$$SOC^{min} \leq SOC(t) \leq SOC^{max}, \tag{3.12}$$

$$P^{ch}(t) \times P^{dis}(t) = 0, \tag{3.13}$$

$$\eta_c P^{ch}(t) \leq min\Bigg(P^{ch}_{max}(t), \bigg(\frac{BC}{100}\Big(SOC^{max} - SOC(t-1)\Big)\bigg)\Bigg), \tag{3.14}$$

$$\frac{P^{dis}(t)}{\eta_d} \leq min\Bigg(P^{dis}_{max}(t), \bigg(\frac{BC}{100}\Big(SOC(t-1) - SOC^{min}\Big)\bigg)\Bigg). \tag{3.15}$$

The equation (3.11) shows that the SOC level at time interval $(t+1)$ depends on the SOC level, charging power, and discharging power at time interval t. Δt is the total duration for time interval t and $t+1$. The equation (3.12) restricts the battery SOC level within the minimum and maximum limits. The charging and discharging of the battery are mutually exclusive, and are represented by the constraint (3.13). The maximum charging and discharging rates of a battery are constrained by equations (3.14) and (3.15), respectively. The electricity price with FDI attack, $\gamma(t)$, can be written as,

$$\gamma(t) = \lambda(t) + norm(\mu, \sigma) \times \lambda(t), \tag{3.16}$$

where, $norm(\mu, \sigma)$ is a Gaussian Noise and $\lambda(t)$ is actual electricity price. The detailed modelling of FDI attack-vector using Gaussian Noise has been described in Chapter 2.

3.3.2 Price and Bill Prediction

The reduced scenario tree of forecasted price scenarios is shown in Figure 3.2. Based on the reduced scenarios, predicted bill, B^P, can be calculated as follows.

$$B^p = \sum_{w} b(w)\pi(w), \tag{3.17}$$

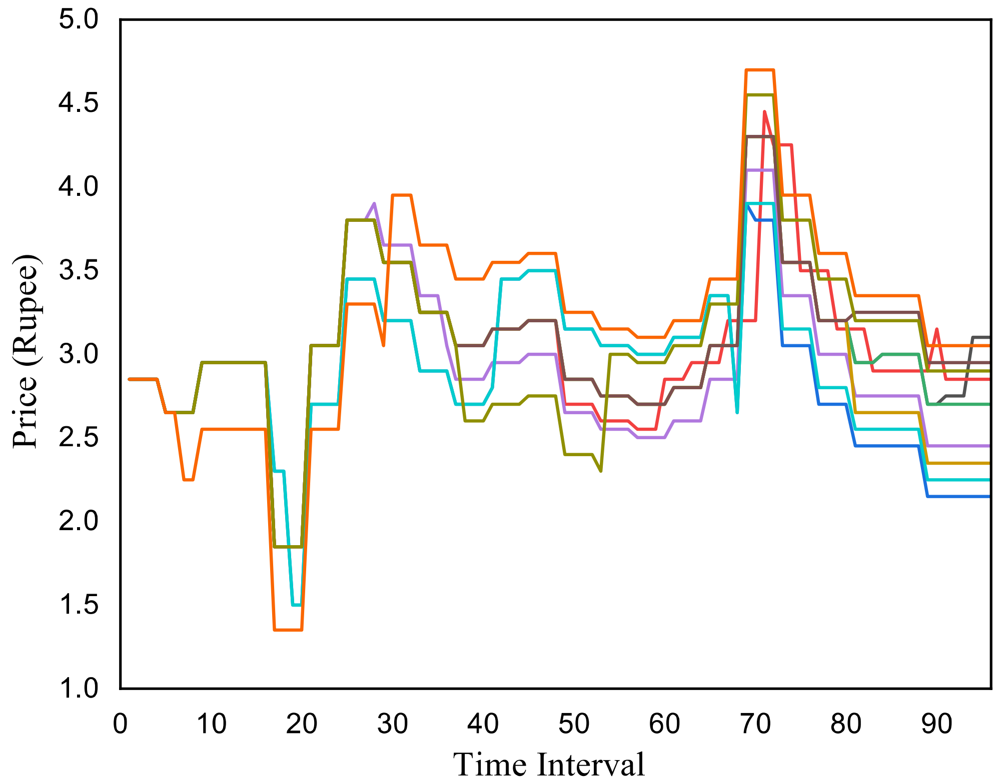

Figure 3.2: Scenario Tree for Bill Prediction

where, $b(w)$ is the energy bill for w^{th} price scenario and $\pi(w)$ is the probability of w^{th} scenario.

3.3.3 FDI Attack Resilient Scheduling

In order to make SHEMS resilient against FDI attack, additional constraints have been introduced in the formulation given in section 3.3.1. These constraints are developed based on the threshold level set by the scheduler. The scheduler develops these thresholds values based on the predicted bill. The difference between the estimated bill, B^P, and the actual bill, B, raises suspicion of a possible attack. If the difference between B^P and B is over the limit then it indicates the probability that the price is under attack. In such cases, the scheduling is done in such a way that it fulfills the following condition.

$$(1-\tau)B^P \leq B \leq (1+\tau)B^P, \tag{3.18}$$

where, τ, is the tolerance set by user.

3.4 Results and Discussion

The proposed system is validated by considering different residential loads, RESs and BSSs. Different types of residential loads, viz. UNLs, SLs, and TDLs, along with their ratings are given in Table 3.1, 3.2 and 3.3 respectively. The specifications of the batteries and components of the test system on the proposed architecture Fig. 3.1 are given in Tables 3.4 and 3.5, respectively. The renewable energy generation from solar PV panel and wind turbine are depicted in Figure 3.3. The RTP decided by utility, and the different expected load variations during 24 hour in 15 mins interval are given in Figure 3.4 and Figure 3.5, respectively. The proposed SHEMS scheme is implemented in GAMS using BARON solver. BARON solves an MINLP problem with global optimality as described in [144], [145]. The status indicated for the proposed model shows optimal solution for the problem. This work considers that the duration of UNLs interval is 15 minutes, which implies that the power consumption by any UNLs over a particular interval remains constant.

Table 3.1: Power Ratings of Unschedulable and Noninterruptible Loads (UNLs)

Sl.No	Appliances	$P_{rated}(kW)$
1	Fan	0.1
2	Compact lamp	0.04
3	Fluorescent Lamp	0.06
4	TV	0.25
5	Mobile/laptop charger	0.05

The duration of interval in case of the SLs is also taken as 15 minutes. It can be noted that once the SL is scheduled and started to run, it can not be interrupted during its operation. The solar radiation, ambient temperature and wind speed of RESs are also taken constant during the RES duration interval of 15 mins as considered by the SHEMS. The price variation during a day is considered on a 15 min interval basis. The SHEMS considers MDL of 5 kW.

Table 3.2: Power Ratings of Schedulable Loads (SLs)

Sl.No	Appliances	$P_{rated}(kW)$
1	EV charger	2.3
2	Grinder	1.5
3	Dish washer	2.1
4	Cloth washer	0.8
5	Well pump	1.5
6	Cloth dryer	2.7

Table 3.3: Power ratings of Temperature Dependant Loads (TDLs)

Sl.No	Appliances	$P_{rated}(kW)$
1	Air conditioner	1
2	Refrigerator	0.5

Table 3.4: Battery Specifications.

Sl.No	Parameter	Rating
1	Capacity	20 Ah
2	Voltage	12V
3	Charging efficiency	95%
4	Discharging efficiency	95%
5	SOC	30-90%
6	Charging current limit	5-20% of rated capacity
7	Discharging current limit	0-20% of rated capacity

Table 3.5: Number of Components in the residential test system

Sl.No	Components	Rating	Count	Total rating
1	Solar PV	0.1 kw	24	2.4 kW
2	Wind turbine	1 kw	2	2 kW
3	Battery	12 v,20 Ah	10 in series	2.4 kW

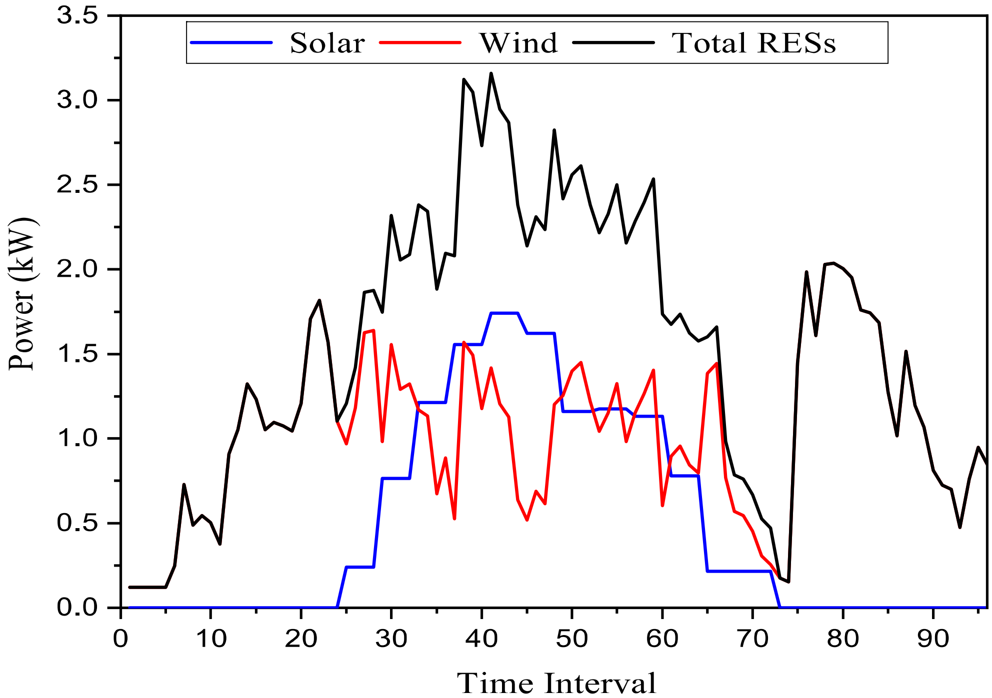

Figure 3.3: RES Generation [1]

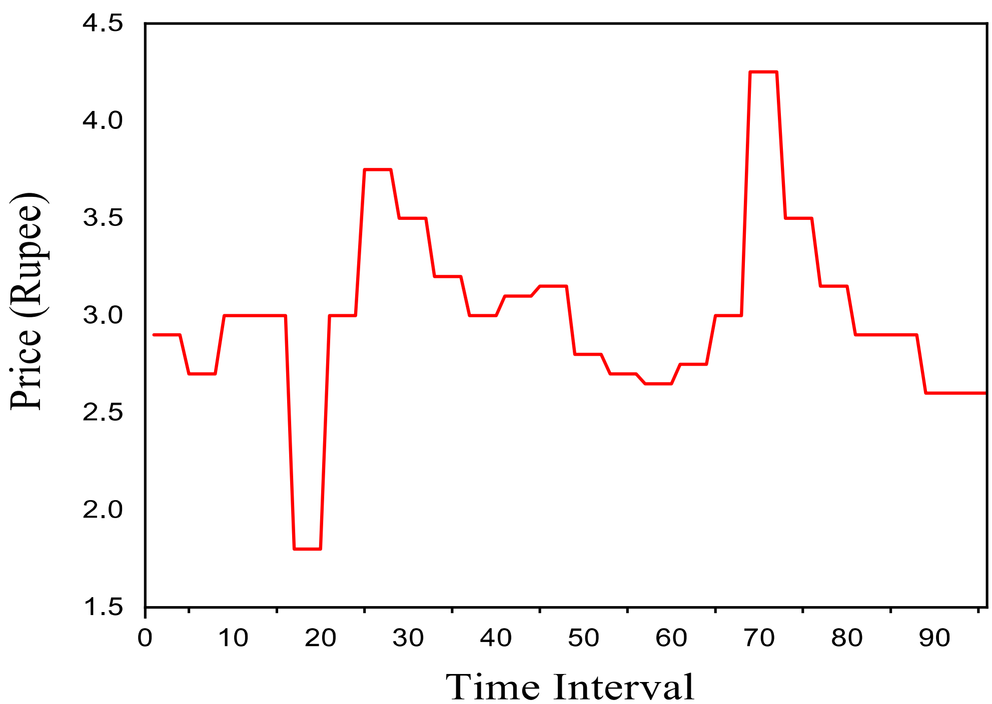

Figure 3.4: Real Time Price (RTP) [1]

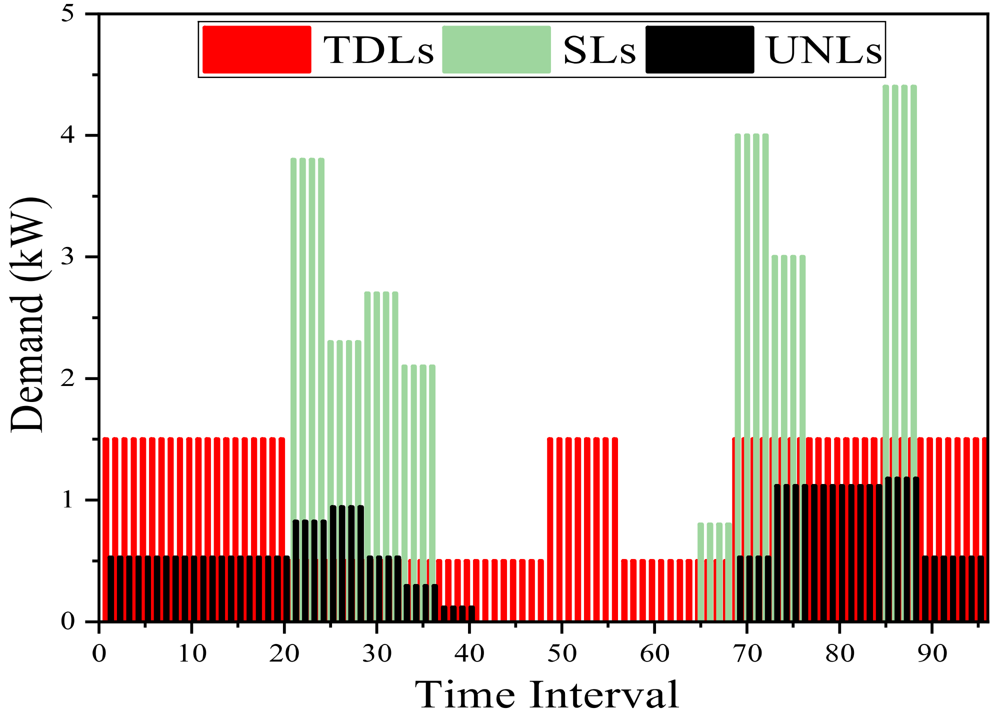

Figure 3.5: Expected load Variations During 24 Hours

3.4.1 Energy Scheduling Considering Battery Degradation Cost

Unscheduled and scheduled load patterns considering renewable energy generation and battery constraints are shown in Figure 3.6. It is observed from Figure 3.6 that the unscheduled demand is having peak during intervals (20-23), (68-75) and (85-88), whereas after scheduling, the peak demand is shifted to the off-peak intervals (1-19), (38-67), (73-81), and (90-96). It is found that the electricity bill for a particular day with unscheduled loads is ₹467.23 where as it is ₹208.14 in the case of scheduled loads. It can be observed from Figure 3.6 that peak demand is shifted to the off-peak demand due to the scheduling under dynamic demand response. This demonstrates that the scheduling shifts the demand from high price periods to low price periods. It can be concluded that SHEMS not only reduce the total electricity bill of a particular day but also reduces the peak demand of the system. Figure 3.7 shows the profile of the total available generation from RESs, power import from the grid and power export to the grid after scheduling. From Figure 3.7, it is observed that the power import by SHEMS is more during the intervals (5-25), (70-76) and (87-96) when generation is low and demand is high. It is also observed that the power export to the grid is more during the high renewable generation periods in the

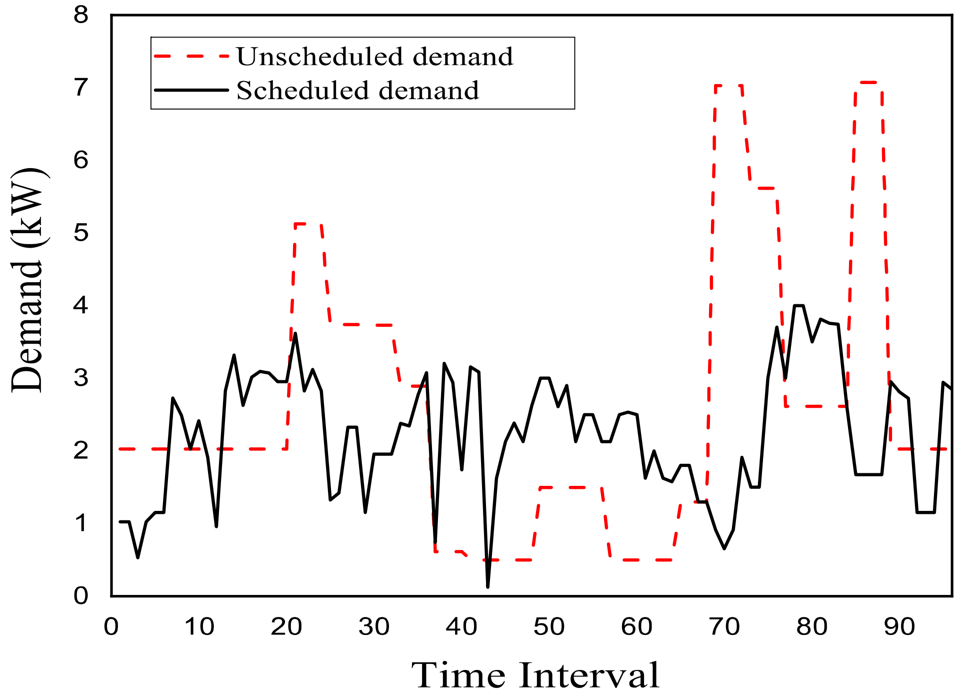

Figure 3.6: Unscheduled and Scheduled Demand

interval (38-45) due to low load demand.

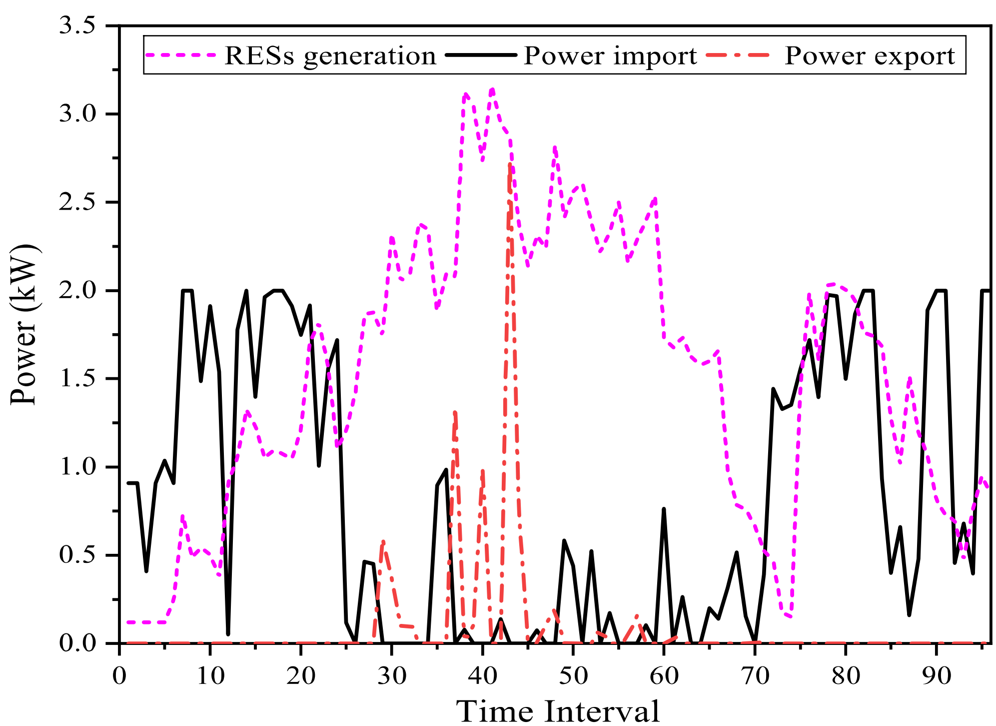

Figure 3.7: RES Generation, Import and Export Power

Figure 3.8 shows the variations of scheduled demand, with and without consideration of battery degradation cost, showing the effect of battery degradation cost on scheduling. It is observed that, when battery degradation cost is considered, the total electricity bill is ₹211.16 which is more than that of without consideration of battery degradation cost. Therefore, it is necessary to consider minimization of both energy cost and as well as battery degradation cost.

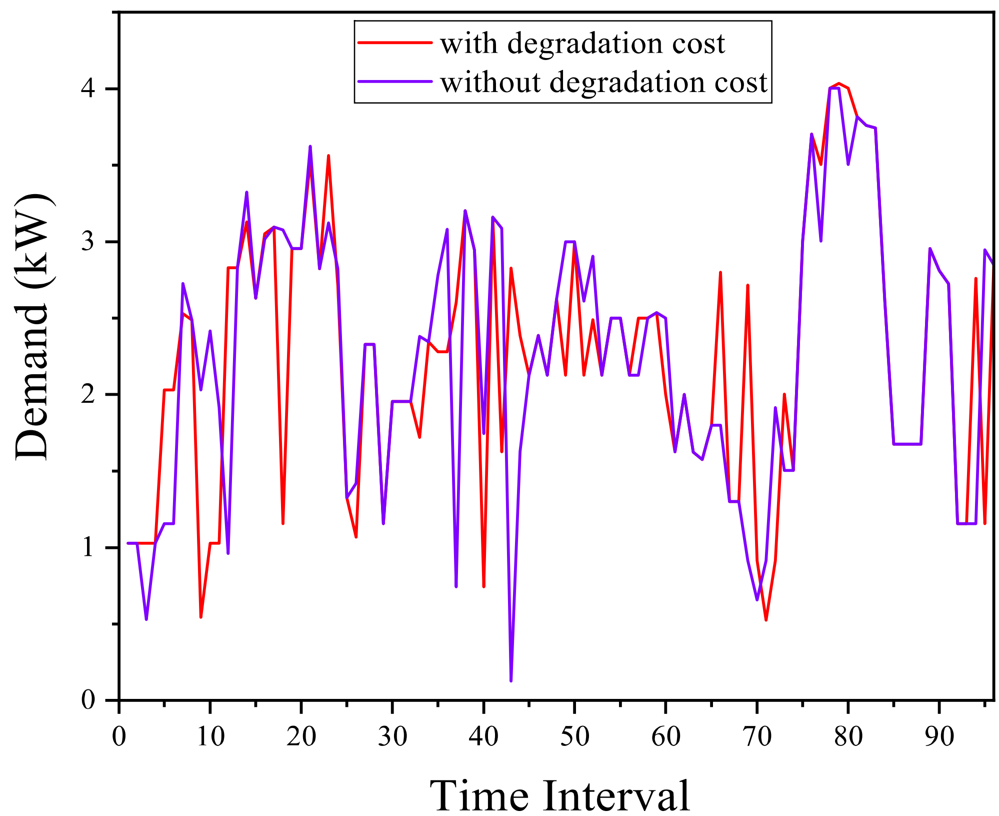

Figure 3.8: Scheduled Demand with and without Battery Degradation Cost

Figure 3.9, shows the power import profile during the 24 hour interval with and without considerations of battery degradation cost. Figure 3.10 shows the profile of power export to the grid. It is observed that higher power export occurs when scheduling is performed without considering battery degradation cost. Figure 3.11 shows the variation of the SOC profile of battery with and without degradation cost. Figure 3.12 shows the charging (+1) and discharging (-1) of battery at different time instants. It can be observed that the battery undergoes more number of charging/discharging cycles when the battery degradation cost is not considered in the problem. Thus, it may be concluded that, without considerations of battery degradation cost, charging/discharging occurs more

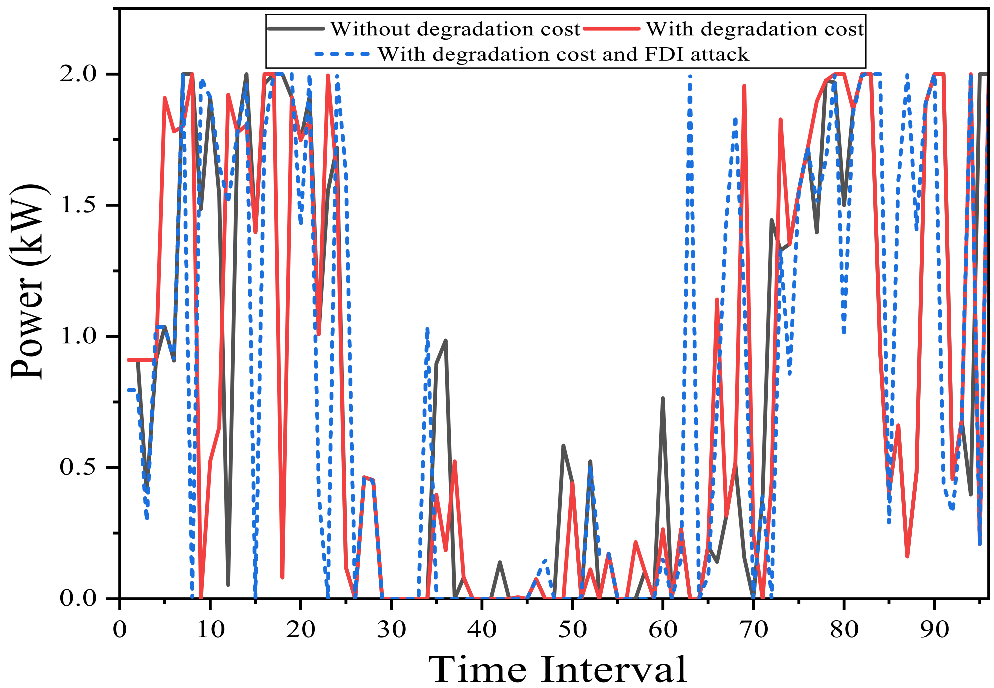

Figure 3.9: Power Import

frequently in a short duration of time which may lead to deterioration the durability and life time of the battery.

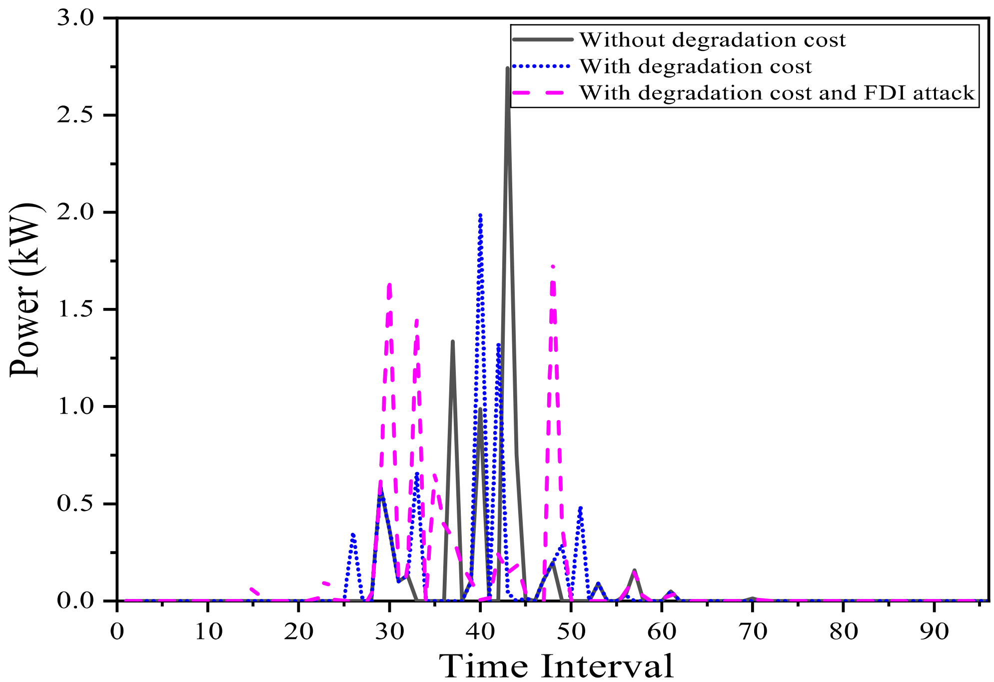

Figure 3.10: Power Export

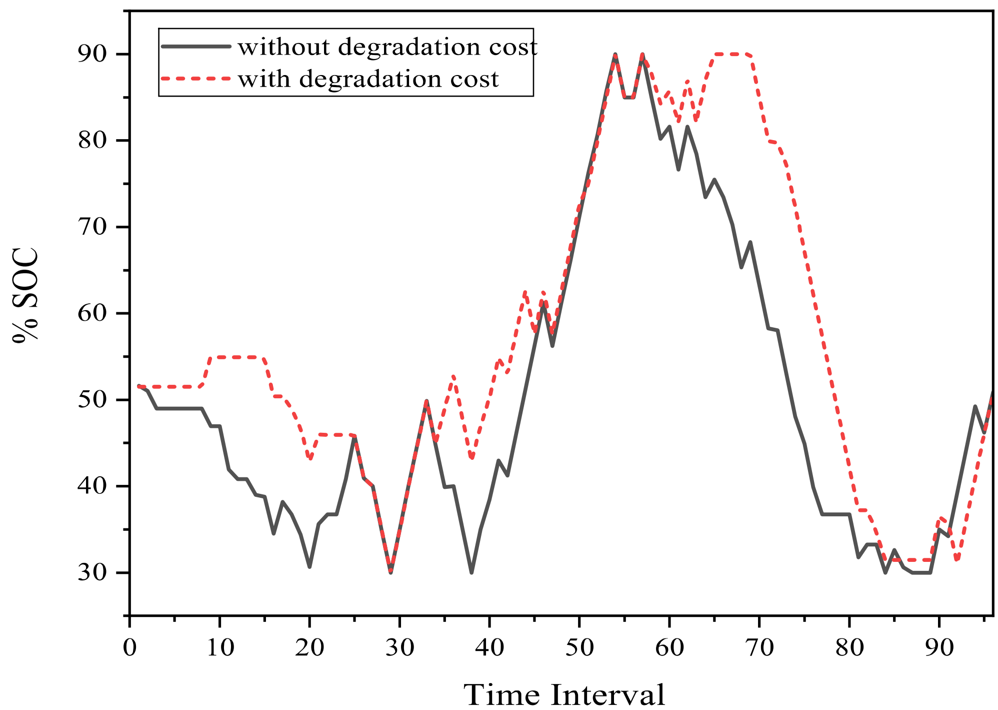

Figure 3.11: SOC with and without Battery Degradation Cost

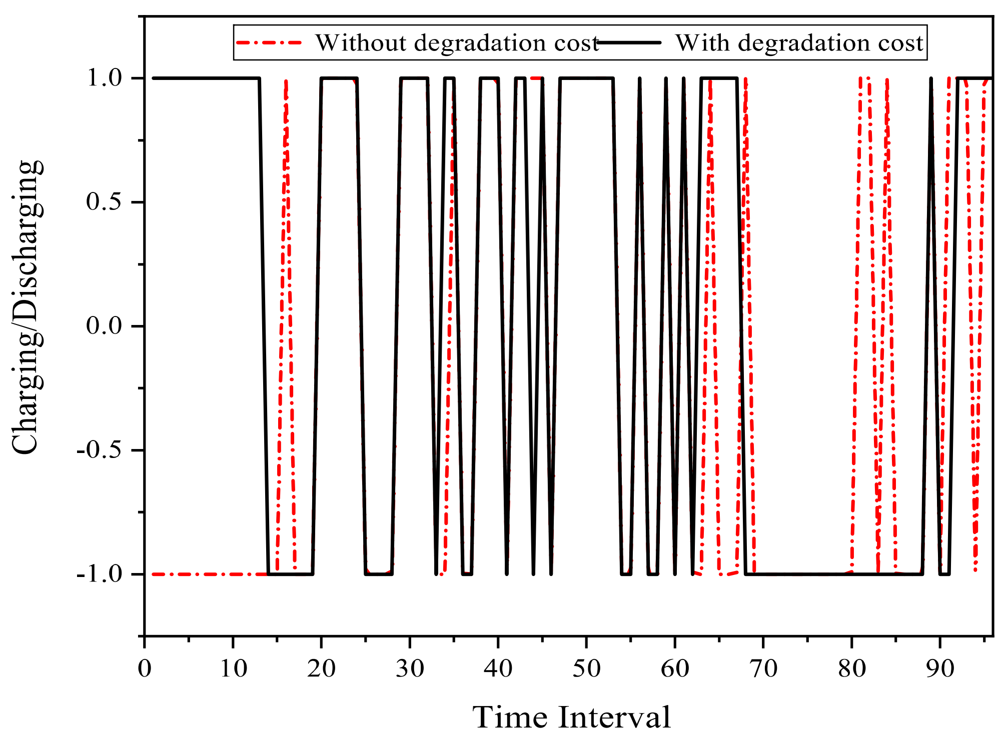

Figure 3.12: Charging and Discharging Cycles with and without Battery Degradation Cost

3.4.2 Energy Scheduling under FDI Attack

In this section, the effects of FDI attack on scheduling is investigated. Figure 3.13 shows variation of the actual price and price after attack over a particular day for the test system. When pricing attack occurs, SHEMS performs scheduling based on the corrupted price data in place of the actual price [146]. Electricity bill is calculated with corrupted price value and without corrupted price value. The electricity bill after scheduling with attack is ₹179.23 and without attack is ₹211.16. If electricity bills are compared, the electricity bill without attack is higher than the bill with attack. So, it is seen from above comparisons that FDI attack can affect the consumer's electricity bills drastically. A corrupted electricity pricing over a duration of time may create a loss or profit to the consumer.

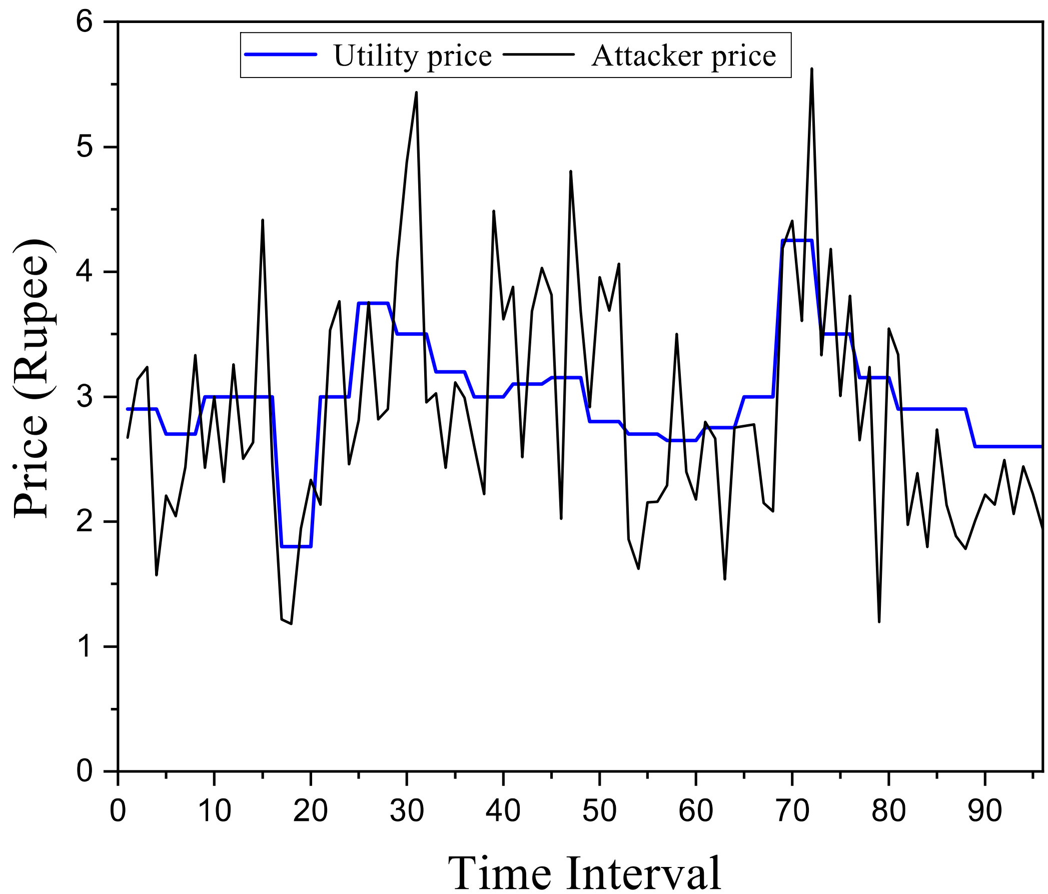

Figure 3.13: Utility Price with Attack

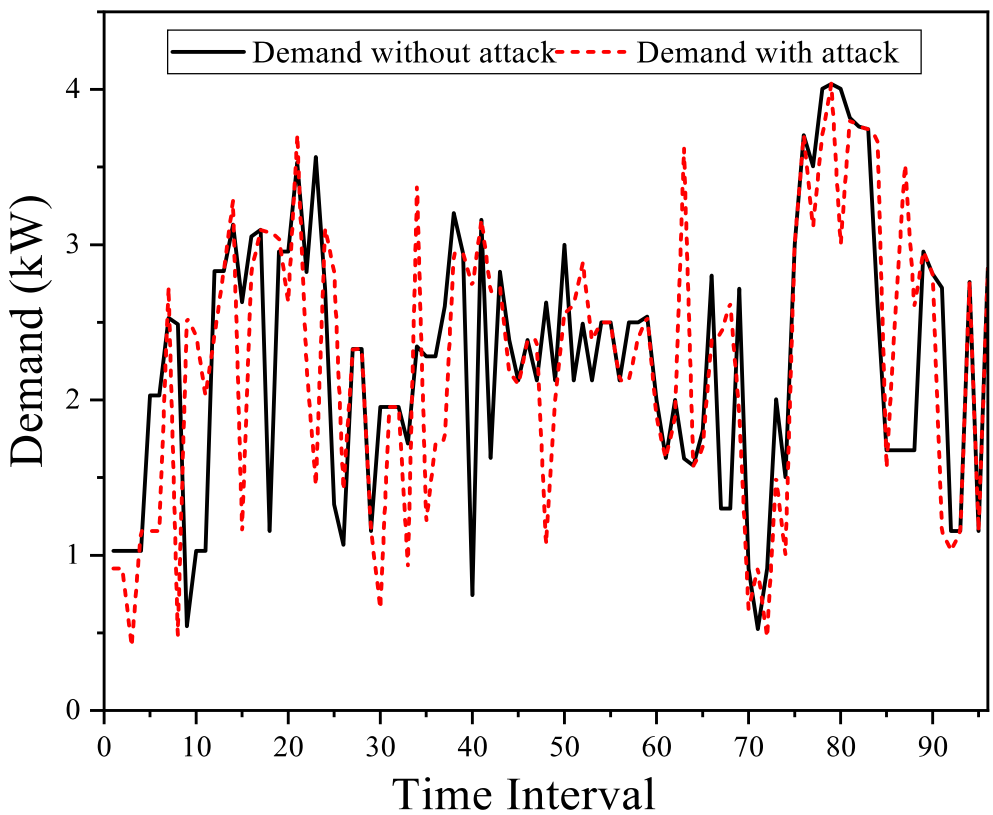

Figure 3.14: Power Demand without and with Attack

Figure 3.14 shows the load consumption pattern with and without pricing attack. The peak demand for both the conditions remains same but it is shifted from one point to another in case of pricing attack. Figure 3.9, shows the power import profiles during 24 hour interval for SHEMS under different conditions. It is observed that under pricing attack the total power import is higher (78.15 kW) as compare to the case when there is no pricing attack (76.99 kW). Figure 3.10 shows the profile of power exports with and without pricing attack, it is observed that higher power export occurs when the FDI attack is in operation.

3.4.3 FDI Attack Resilient Scheduling

This section presents the effects of FDI-attack resilient scheduling algorithm. Figure 3.15 shows the scheduled demand with FDI-attack resilient approach when the scheduling is made under FDI attack. It is observed from Figure 3.15 that power demand patterns are similar in both the cases viz. scheduling without FDI attack and scheduling with

FDI-attack resilience. Figure 3.16 shows the power import with and without FDI-attack resilience. It is confirmed that power import with FDI-attack resilient scheduling is nearly equal to the power import without FDI-attack i.e., with actual pricing data. The electricity bill with FDI-attack resilient scheduling is ₹199.54 while without attack, it is ₹211.16 as given in Table 3.6. From the above comparison, it is observed that SHEMS scheduler should use the FDI-attack resilient scheduling to avoid the effects of FDI attack, as soon as possible in its actual demand scheduling.

Without resilient scheduling, when pricing attack occurs, SHEMS will perform scheduling based on the attacked price data. Thus electricity bill with attacked price will naturally be very low as per the attacker objective. However, with incorporation of resilient scheduling, the electricity bill using the predicted price comes closer to the actual electricity bill obtained (without attacked price), thereby alleviating the effect of FDI attack. This has been validated in details with the help of simulation results as follows,

The Table 3.6 shows the electricity bill without FDI attack, with FDI attack and with resilient constraint are ₹211.16, ₹179.23 and ₹199.54 respectively. The electricity bill difference between with and without FDI attack is ₹31.93 (15.12 %) which is very large. But in FDI attack with resilient constraints and without attack, the electricity bill difference is ₹11.62 (5.5%) which shows that nearly 10% of electricity bill reduces in presence of resilient constraint. That means the proposed resilient scheduling alleviates the effect of FDI attack by nearly 10%.

Table 3.6: Electricity Bill

S.No	Scheduling condition		Electricity Bill (₹)		
			Without FDI-attack	With FDI-attack	With resilience to FDI-attack
01	Without scheduling		467.23	-	-
02	With scheduling	Without battery degradation cost	208.14	-	-
		With battery degradation cost	211.16	179.23	199.54

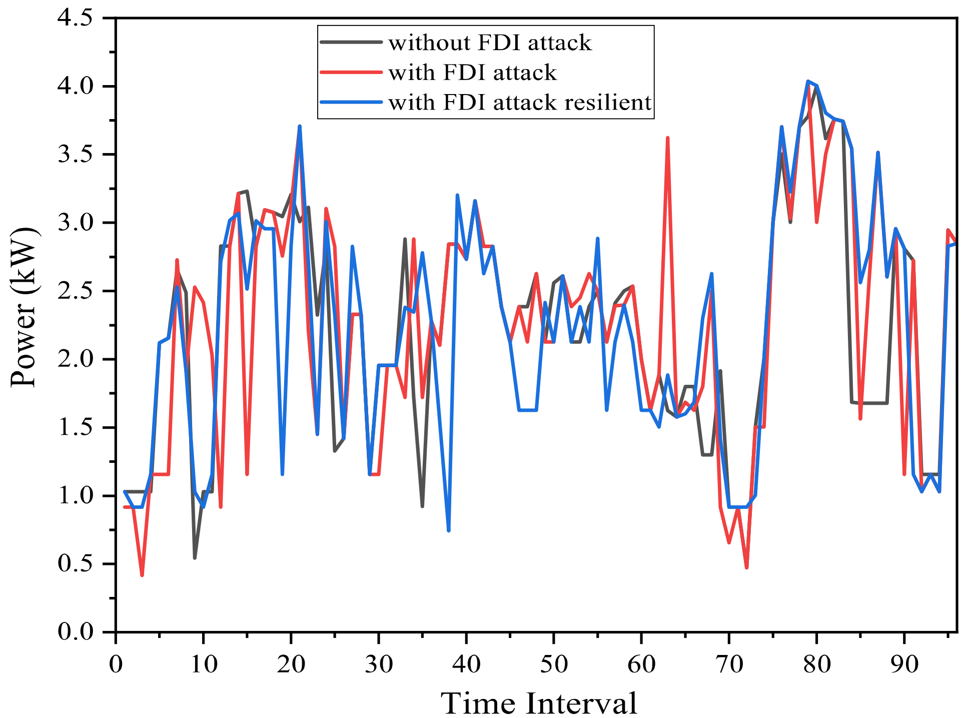

Figure 3.15: Scheduled Demand with and without FDI Attack Resilient

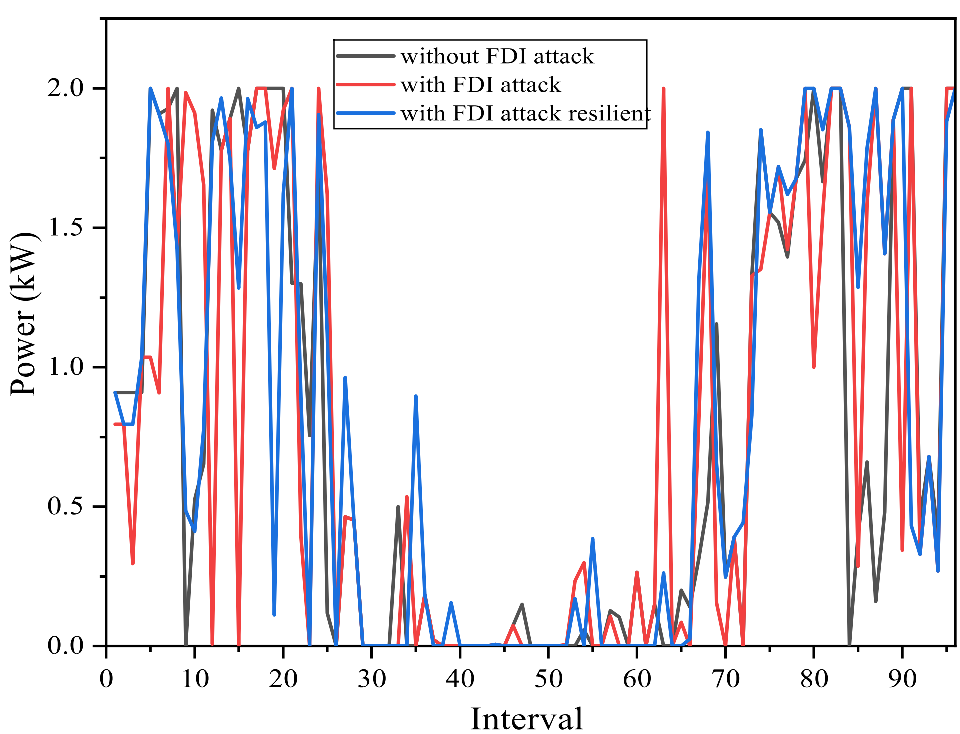

Figure 3.16: Power Import from Grid with and without Resilient

3.5 Summary

In this chapter minimization of the energy cost has been formulated as an optimization problem considering battery degradation cost for a smart home using dynamic demand response. Battery degradation cost depends on Depth-of-Discharge (DOD) and discharging cycle of the battery. It is observed that incorporation of battery degradation cost in the formulation reduces the frequency of charging and discharging of battery.

Further, it is seen that in case of demand scheduling of smart home considering FDI attack, electricity bill and load consumption of the consumer gets affected drastically. Constraints based on the consumer past behaviour have been introduced in the proposed formulation to make scheduling resilient to the FDI attack. The proposed FDI-attack resilient scheduling alleviates the effect of FDI attack.